The Journal of Engineering

The 7th International Conference on Renewable Power Generation (RPG 2018)

IET Journals
The Institution of Engineering and Technology

Development of low translator mass linear Vernier machine for wave energy power take off

eISSN 2051-3305
Received on 29th October 2018
Accepted on 05th December 2018
E-First on 18th June 2019
doi: 10.1049/joe.2018.9304
www.ietdl.org

Mohammad A.H. Raihan[1] ✉, *Nick J. Baker*[1], *Kris J. Smith*[1], *Ahmed A. Almoraya*[1]

[1]*Electrical Power Research Group, School of Engineering, Newcastle University, Newcastle upon Tyne, NE17RU, UK*

✉ *E-mail: M.A.H.Raihan1@newcastle.ac.uk*

Abstract: This article proposes a new topology of double-sided linear Vernier permanent magnet (LVPM) machine with segmented translator structure. A combination of a typical Halbach array consists of two horizontally magnetised permanent magnets (PMs) sandwiched between a salient iron tooth and adjacent vertically magnetised PM pole with the aim of improving its electromagnetic performance. The coreless partitioned translator contributes to a significant reduction in mass and the associated cost. With the aid of finite element analysis (FEA), two LVPM machines with the same PM, and stator volume have been investigated, analysed, and compared. The results imply that the proposed LVPM is capable of producing higher force density, while it exhibits lower cogging force and force ripple compared to its counterpart.

1 Introduction

For wave energy and other applications, there is a demand for linear machines with high force and power density. In linear machines, a simple and robust structure of the translator is preferable, in which the active components such as permanent magnets (PMs) and copper coils can both be mounted in the stator [1, 2].

High power density can be achieved by employing any member of the family of variable reluctance machines. Variable reluctance PM (VRPM) machines share the basic principle of linking flux between sets of PMs and salient teeth [2]. Examples include the Vernier hybrid machine (VHM), flux reversal machine (FRM), and transverse flux machine (TFM) [3, 4]. Those machines generally consist of PM arrays with short pitch that move parallel to the slotted structure as shown in Fig. 1*a*. Alignment and un-alignment between PM arrays and slotted structure produce high forces even for a small displacement, exhibiting the 'magnetic gearing' effect [3, 5]

The TFM arguably can deliver the highest force density in air-cooled applications with low magnet consumption. However, complex 3D flux path, translator mounted magnets, and a thick translator core may cause problems in linear applications and increase the complexity of manufacturing.

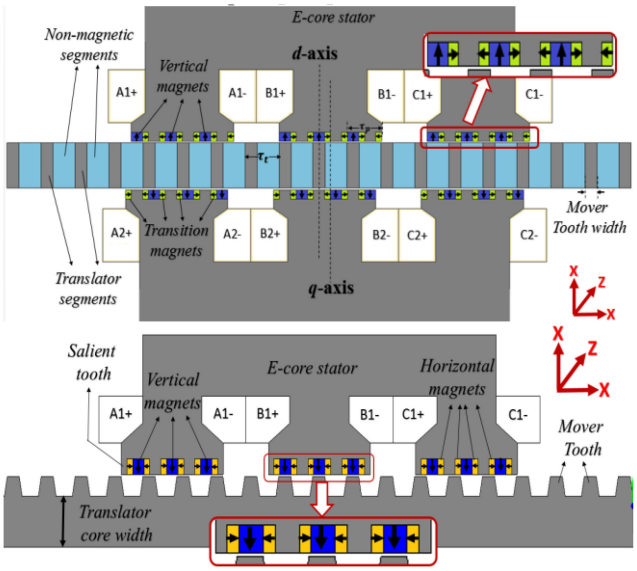

Fig. 1 *Machine topology of*
(a) Design 1, ***(b)*** Design 2

The VHM is known to exhibit high force density similar to the TFM, but with the simple construction of the FRM [6, 7]. The VHM machine has proved to be suitable for low-speed direct drive applications due to high torque or force density, flux reversal/switching characteristics, and inherent magnetic gearing. However, the leakage flux is seen as problematic where only half of the magnets contribute to the useful flux. This phenomenon can limit the back-EMF and produce machines with poor power factor [8]. The nature of the magnets arrangement with alternating polarity in the VHM prevents this machine achieving the same flux produced by its conventional counterpart [8, 9].

The basic design is a development from the Vernier hybrid PM machine topology described in [4, 10]. Alternative PM arrays, such as that proposed in [1], will be investigated here with a view to reducing flux leakage. Fringing flux is further reduced by adopting consequent poles [11], where alternative PMs are replaced with iron teeth.

Linear machines can either have a main flux path through the translator, in the case of a double-sided stator (Fig. 1*a*), or flux traveling along the translator in the case of a single-sided machine (Fig. 1*b*). For the double-sided machine, in order to reduce translator mass, it is possible to adopt a coreless segmented translator [12].

The two topologies of Fig. 1 with the parameters given in Table 1 and the same stator and PM volume will be compared here. In order to verify results a lab prototype has been built and will be tested.

2 Machine topology

2.1 Machine variations

Figs. 2 and 3 show the differing features of the two designs studied.

2.2 Design 2

Figs. 1*b* and 2. show the single-sided linear Vernier PM (LVPM) machine introduced in [1] and defined as *design 2* here. It employs consequent poles and Halbach array to improve the magnetic flux linkage in the phase windings. Like the other Vernier machines, both the PM array and the phase windings are mounted on the salient short stator. The translator has a simple structure of salient

Table 1 Common specifications for the presented machines

Parameter	Value
number of active translator teeth	9
pole pairs per stator tooth	3
air gap length	1 mm
stator pole pair pitch (PPP)	24 mm
stator tooth width	72 mm
translator pitch	24 mm
number of turns per coil	100
translator speed	1.2 m/s
active Translator length	280 mm

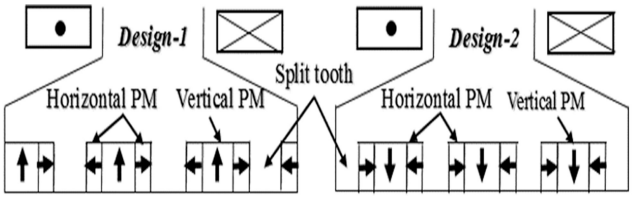

Fig. 2 *PM array orientation for both designs*

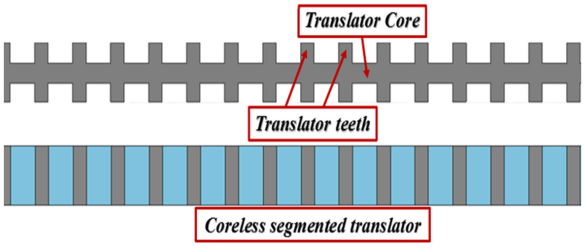

Fig. 3 *Solid translator with core back and segmented translator*

teeth with laminated iron core. The PM array consists of three magnets including the middle magnets, which are vertically magnetised *towards the air gap* and horizontally magnetised transition magnets magnetised *towards the middle PMs* (Fig. 2). Each stator tooth consists of three sets of PM array separated by four salient *split* teeth. In addition, three concentrated windings are adopted for three phases (coils A1, B1, & C1) in the E-core stator separated by 120° electrical. The number pole pairs of the armature winding, $P_{w,}$ can be expressed from [1]

$$P_w = |P_{\mathrm{PM}} - P_s| \tag{1}$$

where P_{s} is the number of active stator teeth and P_{PM} is effective number of PM Pole pairs. Therefore, the magnetic gear ratio, G can be expressed by the following equation

$$G = \frac{P_s}{P_w} \tag{2}$$

Flux passes through the translator core back to the stator via the translator and stator teeth. For this reason, the translator core needs to be thick enough to accommodate the electromagnetic flux.

2.3 Design 1

Fig. 1*a* and 4 present the proposed double-sided linear Vernier PM machine, *design 1*. Two e-core stators are separated from the segmented translator by two identical air-gap regions. Three PM arrays and three salient *split* teeth are mounted on the inner surface of the e-core stator along with the phase windings. Split teeth structure reduces the leakage and fringing flux, while the novel PM array increase the flux density in the machine. Fig. 2 showed the PM array *design 1*, where the magnetisation direction of the PMs are denoted by the arrows shown.

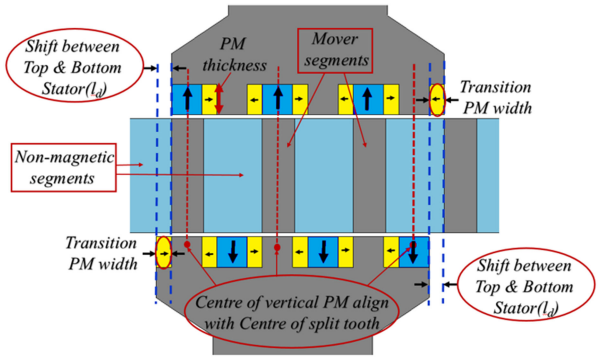

Fig. 4 *Design parameters of the design 1*

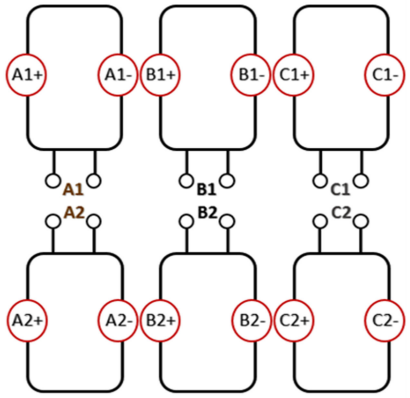

Fig. 5 *Configuration of three phase coils*

Differing from the existing machine mentioned in the previous section, the proposed Vernier machine adopts two horizontally magnetised PMs called *transition* poles magnetised in the *direction of the split teeth*, which is sandwiched between them. Unlike the *design 2* (Fig. 2), the vertical PM *poles* produce the main flux *towards the stator core* and have equal number of split teeth as poles. It is clearly shown in Fig. 4 that the PM array and the split tooth are arranged in such a way that, the centre line of the vertical PM poles from the top stator is aligned with the centre line of the split teeth of the bottom stator and vice versa. The split teeth also act like bidirectional PM poles depending on the position of the mover teeth. The PM flux path is guided by the vertical PM poles. As shown in Fig. 4, there is always a physical offset between the upper and lower stators. The offset must equal the width of a transition pole, magnetised towards the split tooth.

W_{d} is the mechanical displacement between adjacent stator teeth, n is the positive integer, τ_{t} is the translator tooth pitch. To form a balance three phase machine, W_d should satisfy the following equation

$$W_d = \left(1 \pm \frac{1}{3}\right)\tau_t \tag{3}$$

Design 1 consists of three-phase windings, each comprising two concentrated coils from the upper and lower stator connected in series. As Fig. 5 shows, phase A consists of coil A1 and coil A2, phase B consists of coil B1 and coil B2, and phase C consists of coil C1 and coil C2. Since both upper and lower stator teeth under the same phase have the same electrical displacement, the flux variation with translator position is similar for both coils. Fig. 6 shows the flux linkage variation under phase B which produces the back-EMF in both coil B1 and coil B2.

3 Operation principle of machine

The electromagnetic force generation of the proposed Vernier machine is based on the magnetic field modulation between bipolar armature field from the double-sided stator and the translator segments. The field modulation produces nine pole magnetic field

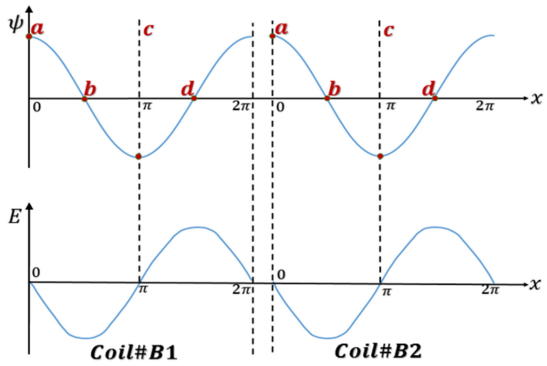

Fig. 6 *Phase B flux linkage and back EMF*

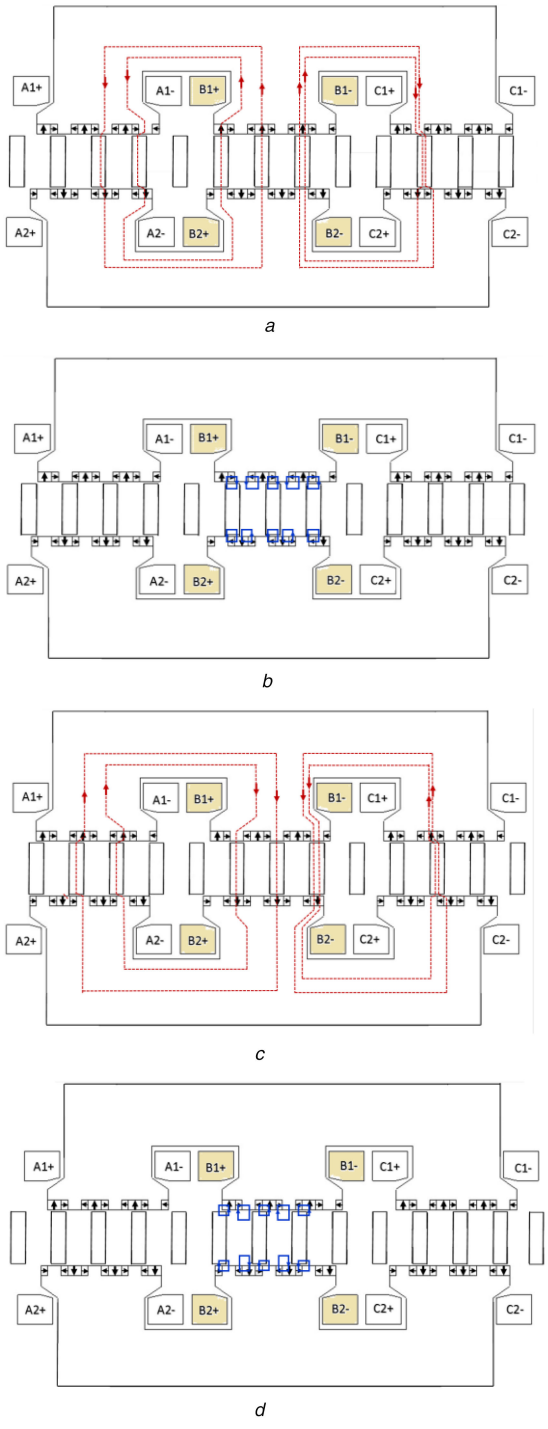

Fig. 7 *Operation principle at different translator positions*
(a) Position a, ***(b)*** Position b, ***(c)*** Position c, ***(d)*** Position d

in each of the two air gaps, which interacts with the stator teeth on both sides and generates a thrust force. The operation principle of the machine can be further demonstrated from Fig. 7 in terms of phase B, by four typical translator positions corresponding to the four points (a, b, c & d) on the phase B flux linkage graph in Fig. 6.

Position a: Translator segments under phase B are aligned with the vertical PM poles of the top stator and split teeth of the bottom stator. As the vertical PM poles from the upper stator produce the main flux, adjacent transition magnets focus their magnetic flux towards the iron split teeth and thus boost the main flux. Vertical PM poles from the lower stator also summate with the active flux. So all the PMs' flux add up together to maximise the active magnetic flux and minimise the leakage flux shown in Fig. 7*b*. Maximum phase B flux linkage and thus minimum back-EMF is generated at this position which can be defined as the *d-axis* operation point.

Position b: Translator segments move quarter of its pitch and are unaligned with the PM poles and split teeth in this position. Almost zero of the phase B flux linkage is produced in this position as the flux leaks between stator poles and translator teeth tips. Therefore, maximum negative phase B back-EMF is produced due to the maximum rate of change in the negative direction. This position is defined as the *q-axis* and maximum thrust force is produced in this position.

Position c: Translator segments move half a pitch relative to position a, to align with the upper split teeth and lower vertical PM poles. This is the negative *d-axis* and negative maximum phase B flux linkage is produced while the back-EMF becomes minimum.

Position d: This position is identical to position b when the translator segments move three-quarter of its pitch relative to position a. Again this is *q-axis* operation and has zero flux linkage under phase B and positive maximum phase B back-EMF are produced.

4 Design and analysis

4.1 Removing translator core-back

Fig. 3 showed the translator with and without core back. A finite element analysis (FEA) on the translator core has been performed to find the optimal core back thickness for maximum average force on the machine. Fig. 8 illustrates an FEA plot of no load flux in the *d*-axis position for *design 1* without a translator core back. With no core back, individual translator teeth are independent components mounted in a non-magnetic structure. This isolated segmented translator has a much reduced mass and improves the flux distribution.

Fig. 9 shows the average force at rated current for different core back thickness. It indicates that the peak average force can be achieved when there is no core back on the translator and the average force seriously decreases when translator core is larger than 14 mm. So, segmented translator is adopted for the proposed machine for maximum force generation.

4.2 Translator tooth width

For maximum thrust force and back-EMF, the segmented translator teeth width is investigated. During design analysis, the translator tooth width has been varied from 4 to 14 mm with increments of 0.5 mm. Fig. 10 shows the results of back-EMF and average force for varying segmented translator teeth width.

The peak-EMF is achieved at 7 mm, while the peak average force is at 8.5 mm. It has been demonstrated in [13] that, thinner tooth saturates when the rated current is applied, and the thrust force reduces very rapidly compared to the reduction of back-EMF with the increase of tooth width. So the optimal translator teeth width has been selected as 8.5 mm for maximum force generation.

4.3 Stator split tooth optimisation

In the proposed Vernier machine, an important factor that has a great impact on back-EMF and cogging force is the *split* teeth

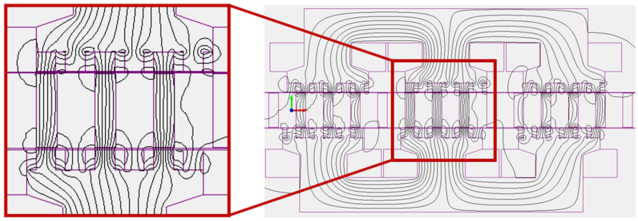

Fig. 8 *No load flux linkage path for design 1*

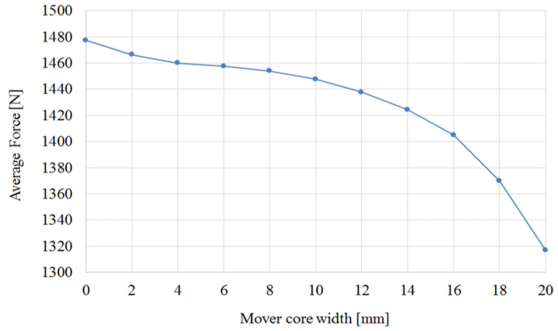

Fig. 9 *Average force variation for translator core width*

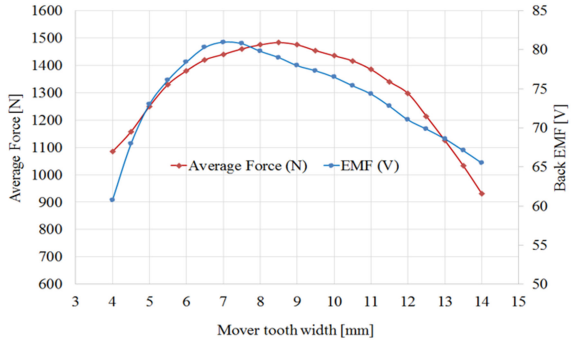

Fig. 10 *Back EMF and average force variation for different translator teeth width*

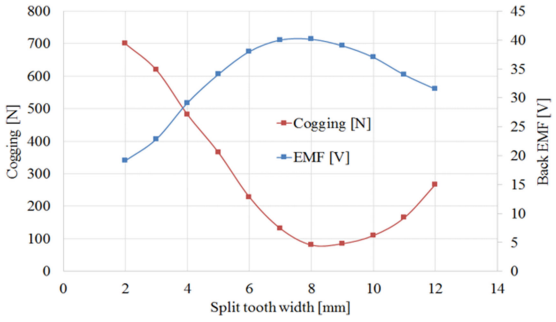

Fig. 11 *Effect of Split tooth width variation on cogging and back EMF*

width. Due to the design restriction, the stator pole pair pitch was constant at 24 mm. It is also assumed that the *pole* width and the split tooth width are identical to get the bipolar flux sinusoidal back EMF. So to change the split teeth width (FT_l), the transition poles width (PM_{lh}) also change to keep the constant stator pole pair pitch (PPP).

$$PM_{lh} = \left(\frac{PPP - FT_l - PM_{lv}}{2}\right) \quad (4)$$

where PM_{lv} is the vertical PM pole width. Fig. 11 shows the variation of peak back-EMF and cogging force ripple with respect to split tooth width. It is clearly shown that 8-mm-split tooth width produce the maximum peak back-EMF with the minimum cogging force ripple.

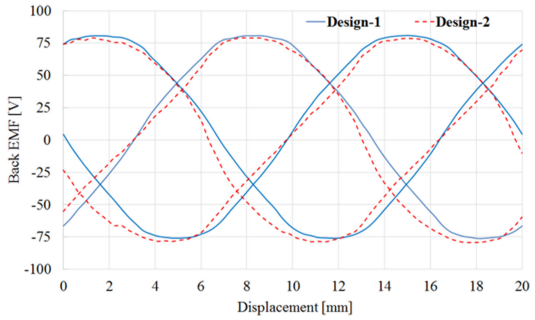

Fig. 12 *Comparison of back-emf for both designs*

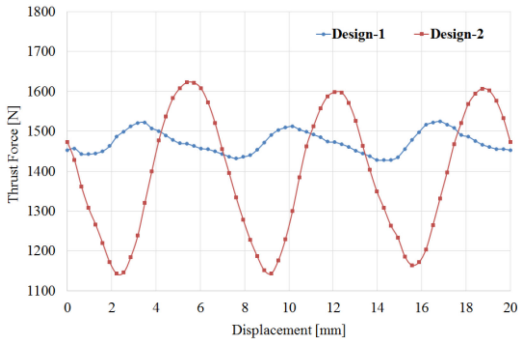

Fig. 13 *Thrust force comparison between design 1 and design 2*

5 Results and comparison

Both designs are based on the common specifications provided in Table 1. The axial length of the single-sided *design* 2 was doubled to match the stator and PM volumes. Both machines have same coil cross-section area, electrical, and magnetic loading.

5.1 Back-EMF

Fig. 12 shows the three-phase back-EMF comparison between the proposed and the existing Vernier machines. Peak no load flux densities are found from FEA for both model, and they are 1.4 and 1.37 T for proposed and existing machine, respectively. For this reason, the peak back-EMF for both machines are very close but the proposed machine has a smoother EMF waveform due to the lower high-order harmonics. Removing the core back helps achieve smoother back-EMF waveform by reducing high-order harmonic spectrum in the proposed Vernier machine.

5.2 Thrust force and cogging

Fig. 13 shows the thrust force waveform for both the machines under same armature current and speed. The proposed machine provides almost 6% higher force for the same rated current. It is also noticeable that, the proposed machine has almost 80% less thrust ripple compared to the existing machine. As the existing machine's translator core size was 35 mm, limited by the stator core back, the translator core saturates at the rated current and produces high thrust ripple.

Fig. 14 shows the cogging force comparison between the two described models. The proposed model has almost 41% lower cogging then the existing Vernier machine.

Table 2 summarise the important design parameters and results for design 1 and design 2.

6 Prototype

A lab prototype of *design 1* with segmented translator is built (Fig. 15*a*) to validate the FEA and compare with the *design 2* (Fig. 15*b* [1]).

7 Conclusion

Here, two force dense LVPM machine topologies are described. Both designs have a Halbach array magnet configuration with

Table 2 Machine parameters and results

Parameters	Design 1	Design 2
Lx [mm]	60.00	120.00
mover total mass [kg]	2.73	16.63
stator mass [kg]	12.42	12.42
PM mass [kg]	1.04	1.04
average Force [N]	1473	1391
force ripple [N]	97	480
back EMF [V]	80.60	79.20
shear stress [kN/m2]	43.84	41.40
force density [kN/m3]	503.90	353.08

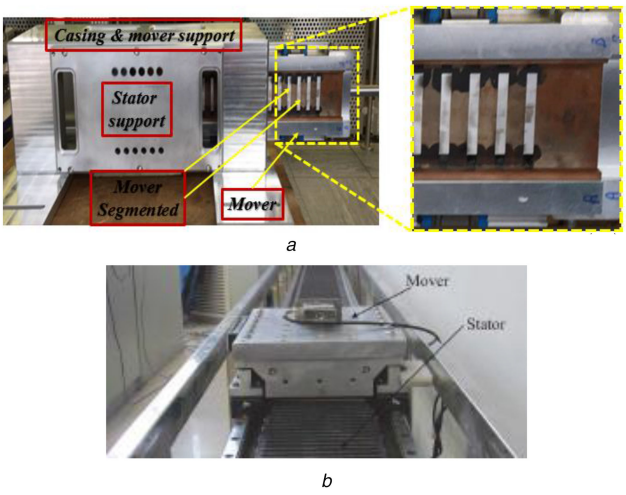

Fig. 15 *Prototype machine*
(a) Design 1, ***(b)*** Design 2, from [1]

consequent poles. The magnet orientation and flux path in the translator are different for a single- or double-sided configuration. A substantial saving of translator mass by employing segmented translator structure is shown. Therefore, the proposed Vernier machine has the potential to offer 30% more force density per machine volume with a similar amount of PM material which is desirable in low-speed direct drive applications. It also offers almost 85% reduction in translator mass which is vital in terms of long-stroke applications like wave energy power take off.

8 Acknowledgment

This work was supported in part by the UK EPSRC under Grant EP/N021452/1.

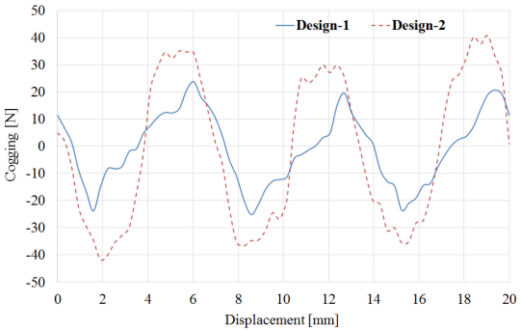

Fig. 14 *Cogging force comparison between design 1 and design 2*

9 References

[1] Ji, J., Zhao, W., Fang, Z., *et al.*: 'A novel linear permanent-magnet Vernier machine with improved force performance', *IEEE Trans. Magn.*, 2015, **51**, (8), pp. 1–10

[2] Bian, F., Zhao, W., Ji, J., *et al.*: 'Analysis of half Halbach array configurations in linear permanent-magnet Vernier machine', *J. Magn.*, 2017, **22**, pp. 414–422

[3] Du, Y., Chau, K.T., Cheng, M., *et al.*: 'Design and analysis of linear stator permanent magnet Vernier machines', *IEEE Trans. Magn.*, 2011, **47**, pp. 4219–4222

[4] Mueller, M.A., Baker, N.J.: 'Modelling the performance of the Vernier hybrid machine', *IEE Proc., Electr. Power Appl.*, 2003, **150**, pp. 647–654

[5] Liu, C., Zhong, J., Chau, K.T.: 'A novel flux-controllable Vernier permanent-magnet machine', *IEEE Trans. Magn.*, 2011, **47**, pp. 4238–4241

[6] Spooner, E., Haydock, L.: 'Vernier hybrid machines', *IEE Proc., Electr. Power Appl.*, 2003, **150**, pp. 655–662

[7] Ching, T.W., Chau, K.T., Li, W.: 'Power factor improvement of a linear Vernier permanent-magnet machine using auxiliary DC field excitation', *IEEE Trans. Magn.*, 2016, **52**, pp. 1–4

[8] Li, D., Qu, R., Li, J., *et al.*: 'Consequent-pole Toroidal-winding outer-rotor Vernier permanent-magnet machines', *IEEE Trans. Ind. Appl.*, 2015, **51**, pp. 4470–4481

[9] Li, D., Qu, R., Lipo, T.A.: 'High-power-factor Vernier permanent-magnet machines', *IEEE Trans. Ind. Appl.*, 2014, **50**, pp. 3664–3674

[10] Baker, N.J., Mueller, M.A., Raihan, M.A.H.: 'All electric drive train for wave energy power take off'. 5th IET Int. Conf. on Renewable Power Generation (RPG), London, UK, September 2016, pp. 1–6

[11] Chung, S., Kim, J., Woo, B., *et al.*: 'A novel design of modular three-phase permanent magnet Vernier machine with consequent pole rotor', *IEEE Trans. Magn.*, 2011, **47**, pp. 4215–4218

[12] Raihan, M.A.H., Baker, N.J., Smith, K.J., *et al.*: 'An E-core linear Veriner hybrid permanent magnet machine with segmented translator for direct drive wave energy converter'. 2017 IEEE Int. Electric Machines and Drives Conf. (IEMDC), Miami, FL, 2017, pp. 1–6

[13] Raihan, M.A.H., Baker, N.J., Smith, K.J., *et al.*: 'A linear consequent pole Halbach array flux reversal machine'. paper presented to 9th IET Int. Conf. on Power Electronics, Machines and Drives (PEMD 2018), Liverpool, 2018